This is an open access article published under a Creative Commons Attribution (CC-BY) License, which permits unrestricted use, distribution and reproduction in any medium, provided the author and source are cited.

ACS OMEGA

Article

Cite This: ACS Omega 2019, 4, 20230−20236

http://pubs.acs.org/journal/acsodf

Reduced to Hierarchy: Carbon Filament-Supported Mixed Metal Oxide Nanoparticles

G. V. Manohara,[†,§] Andrew Whiting,[†] and H. Chris Greenwell*[,‡]

[†]Department of Chemistry and [‡]Department of Earth Sciences, Durham University, Durham DH1 3LE, U.K.

[§]Institute of Mechanical, Process and Energy Engineering (IMPEE), Heriot-Watt University, Edinburgh EH14 4AS, U.K.

Supporting Information

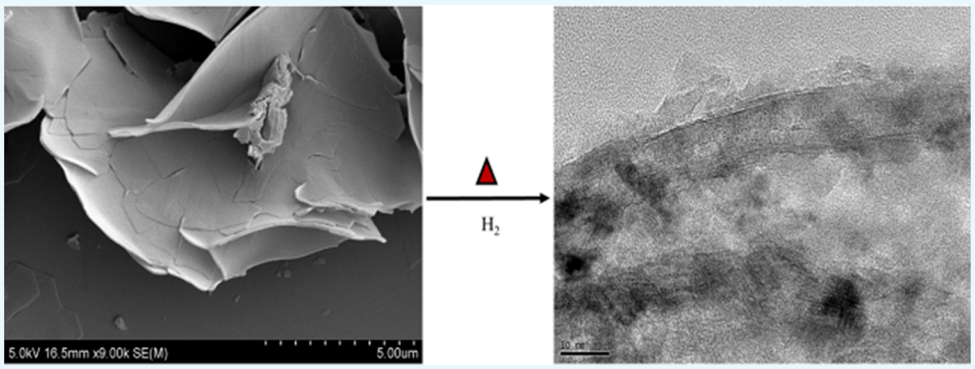

ABSTRACT: We describe a one-pot synthesis method for carbon filament-supported mixed metal oxide nanoparticles. The thermal intracrystalline reaction of adamantanecarboxylate ions confined inside interlayer galleries of layered double hydroxide materials under a reducing atmosphere (H_2) leads to carbon filaments forming in situ within the material. Raman spectroscopy and combined microscopy techniques show the formation of hybrid organic−inorganic carbon filaments with the mixed metal oxide particles interleaved.

1. INTRODUCTION

Intracrystalline reactions are a well-known phenomenon in layered materials.[1] Due to host−guest interactions and the confined structure, dynamics and reactivity of the interlayer region, graphite,[2,3] cationic aluminosilicate clay minerals,[4,5] metal phosphonates,[6−8] and metal chalcogenides[9,10] have all been used to enable and control different kinds of intracrystalline reactions to develop novel functional materials, as well as to control the stereochemistry of reacting interlayer guests.[11,12] The confining interlayer galleries, often only one or two molecule lengths in height, of host layered solids are an ideal place to prepare guest nanomaterials, delivering multifunctionality to the host−guest structure.[13] These hybrid host−guest materials have significant industrial and technological importance.[14−19]

Among layered solids, layered double hydroxides (LDHs) are an increasingly studied class of materials.[20] LDHs have the general formula $[M_{1-x}^{2+}M_x^{3+}(OH)_2]^{x+}(A^{-x/n})\cdot yH_2O$, where, by way of example, M^{2+} = Mg, Co, Ni, Ca, and Zn; M^{3+} = Al, Fe, and Ga; A = anion (organic or inorganic ions); $0.15 \geq x \leq 0.33$; and $0.5 \geq y \leq 1.0$.[21,22] Due to their physicochemical properties, LDHs have gained attention in recent times in the field of catalysis, sorption, polymer nanocomposites, host−guest chemistry, medicine, inter alia.[23] At present, research on LDHs is focused on developing hybrid materials with multifunctional properties, for improved and wider applications.[24−26] Mixed metal oxides (MMOs), prepared by thermal treatment of LDHs, find applications in industrially relevant chemical processes, forming a significant contribution of all heterogeneous base-catalyzed industrial chemistry.[27,28] The properties and the applications of MMOs can be tuned by changing the layered metal hydroxide precursor composition, morphology, and texture.[29] MMOs with insulating, semiconducting, magnetic, and superconducting properties can also be prepared.[30]

LDHs and related MMOs have become widely used owing to their (a) homogeneous distribution of metal ions,[31] (b) diverse tunable composition, (c) easy synthesis protocol, and (d) economic and environmentally benign life cycle. MMOs often encounter sustainability issues due to poor thermal, mechanical, and recycling stability, limiting the number of reuses possible. To exploit these materials at the industrial scale, an immediate challenge is to address these inherent limitations.

Attempts have been made to address catalyst regeneration, including through using catalyst support materials such as graphene oxide (GO), carbon nanotubes (CNT), carbon nanofibers, mesoporous silica, ceramic oxides, inter alia.[32−35]

Received: August 8, 2019
Accepted: October 29, 2019
Published: November 20, 2019

Downloaded via HERIOT-WATT UNIV on January 17, 2020 at 08:35:29 (UTC).
See https://pubs.acs.org/sharingguidelines for options on how to legitimately share published articles.

© 2019 American Chemical Society

DOI: 10.1021/acsomega.9b02534
ACS Omega 2019, 4, 20230−20236

These supported MMOs are found to be better than unsupported MMOs for various applications such as gas adsorption, organic conversions, and electrode materials for batteries and supercapacitors.[36−42] Generally, all these methods are multistep and add significant cost to the life cycle of the materials. Moreover, all these supports are provided as additives during/after the synthesis and result in less even distribution of the catalyst on the support. To overcome this, it is of importance to design and develop a novel method of synthesis where the catalyst is coformed with the support material. Additionally, if the support comes within the LDH, the synthesis process will become more sustainable.

Recently, diamondoids (molecules based on the adamantane structure) and their derivatives have been successfully incorporated inside carbon nanotubes (CNTs) and converted in situ into carbon nanowires/nanochains.[43,44] Here, we report the synthesis of adamantanecarboxylate intercalated Mg-Al LDHs and successful conversion of the material into carbon filaments with supported mixed metal oxide particles. Mg-Al LDHs intercalated with adamantanecarboxylic acid were synthesized by employing an efficient one-pot protocol as described in our previous paper showing excellent thermal stability.[45]

2. RESULTS AND DISCUSSION

The synthesized adamantanecarboxylate was characterized by powder X-ray diffraction (PXRD), with a typical diffraction pattern shown in Figure S1 (Supporting Information). The *d* spacing of 20.6 Å corresponds to a bilayer arrangement of adamantanecarboxylate ions in the interlayer space.[46] Higher order reflections of the 20.6 Å basal spacing are at 10.2, 6.8, and 4.1 Å. The intercalated adamantanecarboxylate anions were further characterized by infrared (IR) and solid-state ^{1}H and ^{13}C nuclear magnetic resonance (SS-NMR) spectroscopies. The IR spectrum (see Figure S2, Supporting Information) shows carboxylate (COO^{-}) stretching vibrations at 1517 and 1395 cm^{-1} and vibrations due to CH_2 and CH bond stretching at 2900 and 2847 cm^{-1}, respectively. The broad absorption feature centered around 3400 cm^{-1} is due to hydrogen-bonded metal hydroxide group O−H stretching and hydrogen-bonded intercalated water.[47] The ^{1}H SS-NMR spectrum of the sample (shown in Figure S3, Supporting Information) shows a sharp peak at 1.01 ppm corresponding to the CH_2 protons of the adamantane ring and a broad peak at 1.74 ppm from CH protons of the adamantane ring.[46] The other two peaks at 3.80 and 4.69 ppm are due to the protons of the intercalated water in the interlayer region and the hydroxyl groups in the metal hydroxide layer, respectively. The ^{13}C NMR spectra of Mg-Al-adamantanecarboxylate (Figure S4, Supporting Information) shows four sharp peaks in the low field region at 29.5, 37.3, 40.6, and 42.8 ppm due to the four different carbon environments present in the adamantane group. The peak at 186.98 ppm is due to the carbon of the carboxylate group in the adamantanecarboxylate.[46]The analyses confirm the successful preparation of the adamantanecarboxylate Mg-Al LDH material.

The resultant adamantanecarboxylate Mg-Al LDH material was converted into carbon filaments with supported Mg-Al MMO material by calcining the LDH at 600 °C under a reducing atmosphere of H_2 gas. The PXRD pattern of the resultant carbon-supported MMOs (Figure 1) shows the reflections at 6.40 Å (13.81° 2θ), 2.54 Å (35.2° 2θ), 2.44 Å (36.9° 2θ), 2.10 Å (42.89° 2θ), and 1.49 Å (62.30° 2θ).

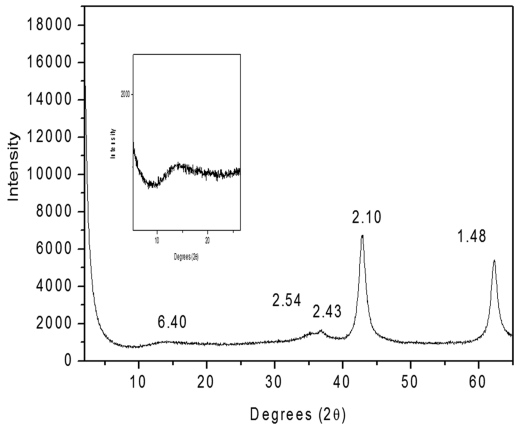

Figure 1. PXRD pattern of the hybrid material generated from reductive decomposition of adamantanecarboxylate intercalated Mg-Al LDH. The *d* spacing values are in Å.

Generally, the thermal decomposition of a typical Mg-Al LDH would be expected to show crystalline MgO peaks in the PXRD pattern as the material phase separates to give MgO and amorphous aluminum phases, followed by reflections indicating spinel formation at higher temperature.

Thermally decomposed intercalated anions generally escape as gases, depending on the nature of the anion (e.g., carbonate readily forms CO_2). In the present case, the reflection at 2.44 Å (36.9° 2θ), 2.10 Å (42.89° 2θ), and 1.49 Å (62.30° 2θ) correspond to 111, 200, and 220 planes of the MgO phase, respectively, although these are atypically broadened.[48] The reflection at 6.40 Å (13.81° 2θ) and 2.54 Å (35.2° 2θ) are unusual for MMOs formed from LDHs, and the 6.4 Å reflection is closely matching with that of a graphite oxide peak, vide infra. The origin of this peak could also be from the formation of the hybrid compound involving MMOs and carbonaceous material suggesting incomplete removal of the anion.[49]

The IR spectrum of the reduced MMO material is given in Figure S5 (Supporting Information) and shows vibrations at 3391, 2982, 2971, 2892, 2648, 1640, and 1394 cm^{-1}. Inorganic LDH-based MMOs formed under similar conditions show no stretching or bending modes in the range of 4000−1000 cm^{-1} in the IR region and show metal−oxygen (M−O) vibrations and breathing modes below 1000 cm^{-1}.[50] The absorptions at 2982 and 2892 cm^{-1} can be assigned to the CH_2 and CH stretching of hydrocarbons, respectively. The broad feature centered around 3390 cm^{-1} is due to hydrogen-bonded hydroxyl group stretches. The vibration at 1640 cm^{-1}may be due to C=C stretching. Figure S5 further shows three distinct vibrational modes in the C−H region (2982, 2971, and 2892 cm^{-1}) as opposed to the two in the parent LDH (2900 and 2847 cm^{-1}). There is shift in the IR frequency of CH_2 and CH vibration from 2900 to 2982 cm^{-1} and from 2847 to 2892 cm^{-1} upon conversion from LDH to MMOs, indicating the change in the nature of the adamantanecarboxylate. The IR spectrum further confirms the presence of hydrocarbon in the resultant MMO material. These observations, taken together, indicate retention and conversion of intercalated adamantanecarboxylate ions in the narrow galleries of hydroxide sheets under reductive calcination.

Solid-state ^{13}C and ^{1}H NMR techniques were employed to further elucidate the structure of the MMO material. The ^{13}C NMR spectrum (Figure 2a) shows two peaks at 33.5 and 126

DOI: 10.1021/acsomega.9b02534
ACS Omega 2019, 4, 20230−20236

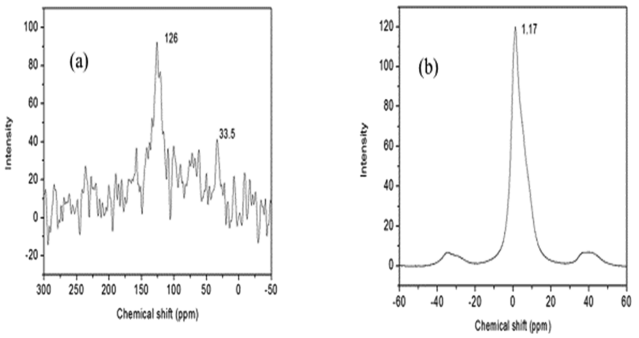

Figure 2. (a) ^{13}C and (b) ^{1}H NMR spectra of the hybrid material generated from reductive decomposition of adamantanecarboxylate intercalated Mg-Al LDH.

ppm, and the peak at 33.5 ppm indicates the presence of sp^3carbon atoms. The peak at 126 ppm is due to sp^2 carbon and is attributed to aromatic or alkene bonding. The ^{1}H NMR spectrum (Figure 2b) shows a very broad peak centered at 1.17 ppm and tailing until 15 ppm. As such, it is difficult to assign protons to any specific functional groups. The center of the peak, 1.17 ppm, is in between the methyl R−CH_3 and methylene R−CH_2−R proton signals. The ^{27}Al NMR spectra of the sample show two peaks at 9.14 and 70.69 ppm in the ratio of 3:2 (Figure S6, Supporting Information). The peak at 9.14 ppm corresponds to Al ions in an octahedral environment, and the peak at 70.69 ppm corresponds to the tetrahedral environment. The transition of Al in the MMOs from octahedral to tetrahedral sites is expected during calcinations and has been reported previously for similar LDH materials.[51]

The MMO material formed during reductive calcination was further characterized with Raman spectroscopy (Figure 3),

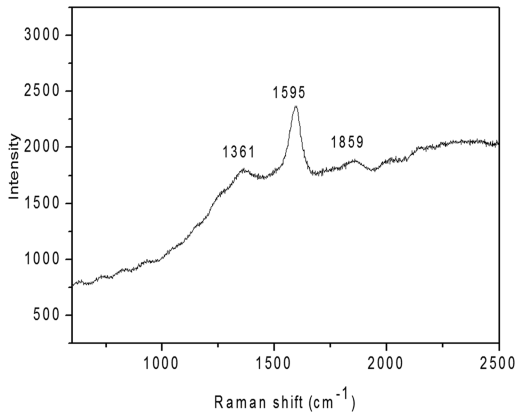

Figure 3. Raman spectrum of hybrid material generated from reductive decomposition of adamantanecarboxylate intercalated Mg-Al LDH.

showing the characteristic G and D bands for carbon materials at 1595 and 1361 cm^{-1}, respectively. The intensity of the G band is higher than that of the D band, indicating graphitic oxide-type carbon, rather than the reduced graphite oxide.[52] An interesting feature of the Raman spectrum is the band at 1859 cm^{-1}, which is associated with linear carbon chains/wires.[13] The Raman spectra suggest that some of the confined intercalated adamantanecarboxylate ions have transformed into a material similar to carbon chains/wires under the reducing atmosphere.

Zhang et al. have tried to convert adamantane molecules into diamond nanowires under a reducing atmosphere (H_2), and the reaction was found to be unsuccessful due to unfavorable energetics of the reaction.[45] The authors predicted that to convert adamantane into linear carbon chains, less stable derivative of diamondoids, for example, carboxylic acids, could be used as starting materials. Here, the adamantanecarboxylate intercalated LDH calcined under the reducing atmosphere is, in part, behaving as predicted by the work of Feng et al.[44]

Scanning electron microscopy (SEM) images of the resultant MMOs are given in Figure 4. SEM images clearly show two different particle types, having distinct morphologies. The MMOs, with nanometer dimensions, can be seen dispersed on aggregate bundles of carbon wires/chains (as shown in the arrows). This again shows the formation of the layered hydroxides as MMOs and intercalated adamantanecarboxylate ion as the carbonaceous support.

Electron microscopy was used to further study the hybrid organic−inorganic nature of the MMOs and the transformed intercalated adamantanecarboxylate ion. The carbon chains/wires suggested in the Raman spectra were elucidated further by high-resolution transmission electron microscopy (HRTEM) images, as shown in Figure 5.

The MMO aggregates/nanoparticles have dimensions of approximately 20−50 nm as shown in Figure 5b. The large fibrous natured materials observed along with MMOs in Figure 5b are carbon filaments originated from transformation of intercalated adamantanecarboxylate ions. The individual carbon filaments appear to be stacked together to form a bundle, having a diameter of around 10 nm. The shape and nature of the resultant carbon upon transformation of adamantanecarboxylate ion is similar to the one observed for diamondoids in the literature.[43,44] Careful observation of these filaments reveals the thickness of subunits to be around 0.3 to 0.4 nm. The highlighted circular objects in Figure 5d correspond to MMO nanoparticles sitting on either side of the resultant carbon chains/wires (highlighted with straight lines). This observation is similar to the one observed in the SEM images (Figure 4). This indicates that the narrow galleries of LDHs facilitated the growth and transformation of intercalated adamantanecarboxylate into low dimensionality carbon structures (sheets/chains). At the same time, the layered hydroxides are converted to MMOs resulting in the formation of hybrid composite. For comparison, TEM images of the parent LDH are given in Figure S7 (Supporting Information) and show the large anisotropic layers of the organo-LDH material.

The elemental composition of the MMOs was determined by energy-dispersive X-ray (EDX), with the results shown in Figure S8 (Supporting Information). The MMO Mg/Al ratio is almost equal to 2, as observed in the parent LDH precursor material. The resultant hybrid shows that Mg and C have near equal proportions. The peaks due to Cu originate from the grid used to mount the sample on for analysis. The distribution of various elements in the resultant nanocomposite was mapped using a scanning transmission electron microscopy (STEM) technique, as shown in Figure 6. The distribution of Mg and C appears almost homogeneous across the material analyzed. However, the distribution of Al suggests that it has segregated into pockets.

DOI: 10.1021/acsomega.9b02534
ACS Omega 2019, 4, 20230−20236

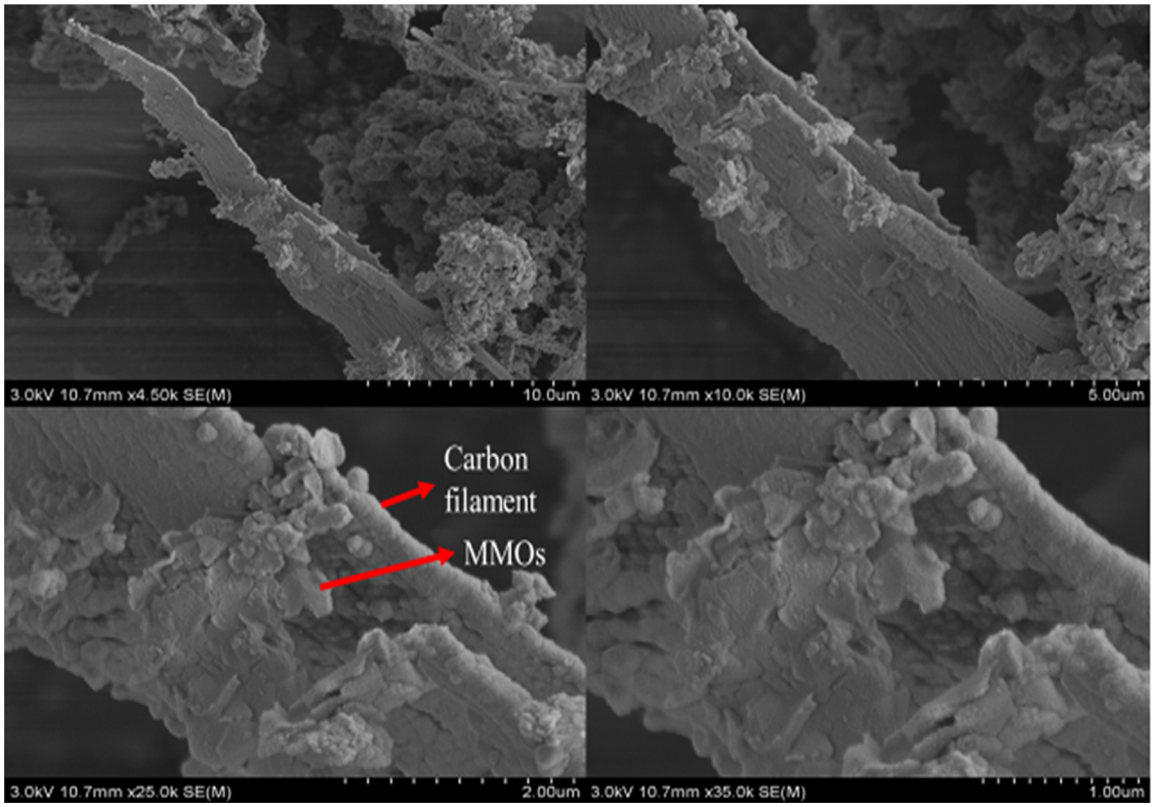

Figure 4. SEM images of the hybrid material generated from reductive decomposition of adamantanecarboxylate intercalated Mg-Al layered double hydroxide (resultant nanocarbon wires/chains and MMOs are shown by arrows).

3. CONCLUSIONS

In summary, we have successfully transformed an adamantanecarboxylate intercalated Mg-Al LDH into a hybrid MMO material through reductive calcination. The intercalated adamantanecarboxylate ion appears to have transformed under hydrogen reduction into carbon filaments, interwoven inside the confining galleries of the layered double hydroxides. The resultant carbon filaments are supporting the MMO materials and offer a potential facile route to high-surface-area hierarchical carbon-supported nanoparticles with basic surface sites.

4. EXPERIMENTAL SECTION

4.1. Synthesis. All reagents, $Mg(OH)_2$, $Al(OH)_3$, and 1-adamantanecarboxylic acid were purchased from Sigma-Aldrich and used as received. Deionized water (18 MΩ cm resistivity, Millipore water purification system) was used throughout the experiment. Adamantanecarboxylate intercalated Mg-Al (Mg/Al =2) was synthesized by employing the cohydration method. In a typical experiment, a stoichiometric amount of $Mg(OH)_2$, $Al(OH)_3$, and 1-adamantanecarboxylic acid (Al/adamantanecarboxylate =1) was taken in 100 mL of water. The reaction mixture was stirred at room temperature for an hour to get a homogeneous mixture. The resultant reaction mixture was transferred to a Parr high-pressure vessel and hydrothermally treated at 150 °C for 24 h. The resultant LDH was recovered by filtration followed by drying at 65 °C for overnight. The hybrid organic−inorganic nanocomposite of MMOs and linear carbon chains/wires was synthesized by reductive decomposition of Mg-Al-adamantanecarboxylate LDH under H_2. In a typical experiment, 1 g of LDH was loaded into a quartz tube and subjected to decomposition at 600 °C under a hydrogen atmosphere. The ramp rate was kept at 5 °C min^{-1}, and the flow of H_2 was fixed at 100 mL min^{-1}. Once the desired temperature was reached (600 °C), the sample was held at that temperature for 4 h. The sample was cooled down without any control on the cooling rate.

4.2. Characterization. Powder X-ray diffraction (PXRD) data was collected using a Bruker D8 Advance diffractometer (θ−2θ scan, Cu Kα radiation, λ = 1.541 Å). Data was collected at a continuous scan rate of 2° 2θ min^{-1} between 2 and 70° 2θ. Samples were gently ground powders and pressed into sample holders. Infrared (IR) spectroscopy analyses of the samples were recorded in the reflectance mode using a PerkinElmer Spectrum 100 FT-IR spectrometer in the attenuated total reflectance (ATR) mode. Ground powder samples of the LDH materials were used. The C, H, and N analyses on the LDH samples were carried out by the Microanalysis service within the Chemistry Department, Durham University. Approximately 3 mg of sample was placed in a tin capsule and combusted in a high oxygen environment at 950 °C using an Exeter Analytical CE-440 elemental analyzer calibrated with acetanilide. Solid-state nuclear magnetic resonance (NMR) studies (^{1}H and ^{13}C) were carried out using a Varian VNMRS spectrometer in the Solid State NMR facility at the Department of Chemistry, Durham University. Raman spectra were recorded using a Jobin Yvon Horiba LabRAM spectrometer using Nd:YAG (532 nm) laser excitation. Transmission electron microscopy (TEM), high-resolution TEM (HRTEM), and scanning electron microscopy (SEM) were carried out at the G. J. Russell Electron Microscopy facility, Department of Physics, Durham University. The surface morphology of all the samples was characterized

DOI: 10.1021/acsomega.9b02534
ACS Omega 2019, 4, 20230−20236

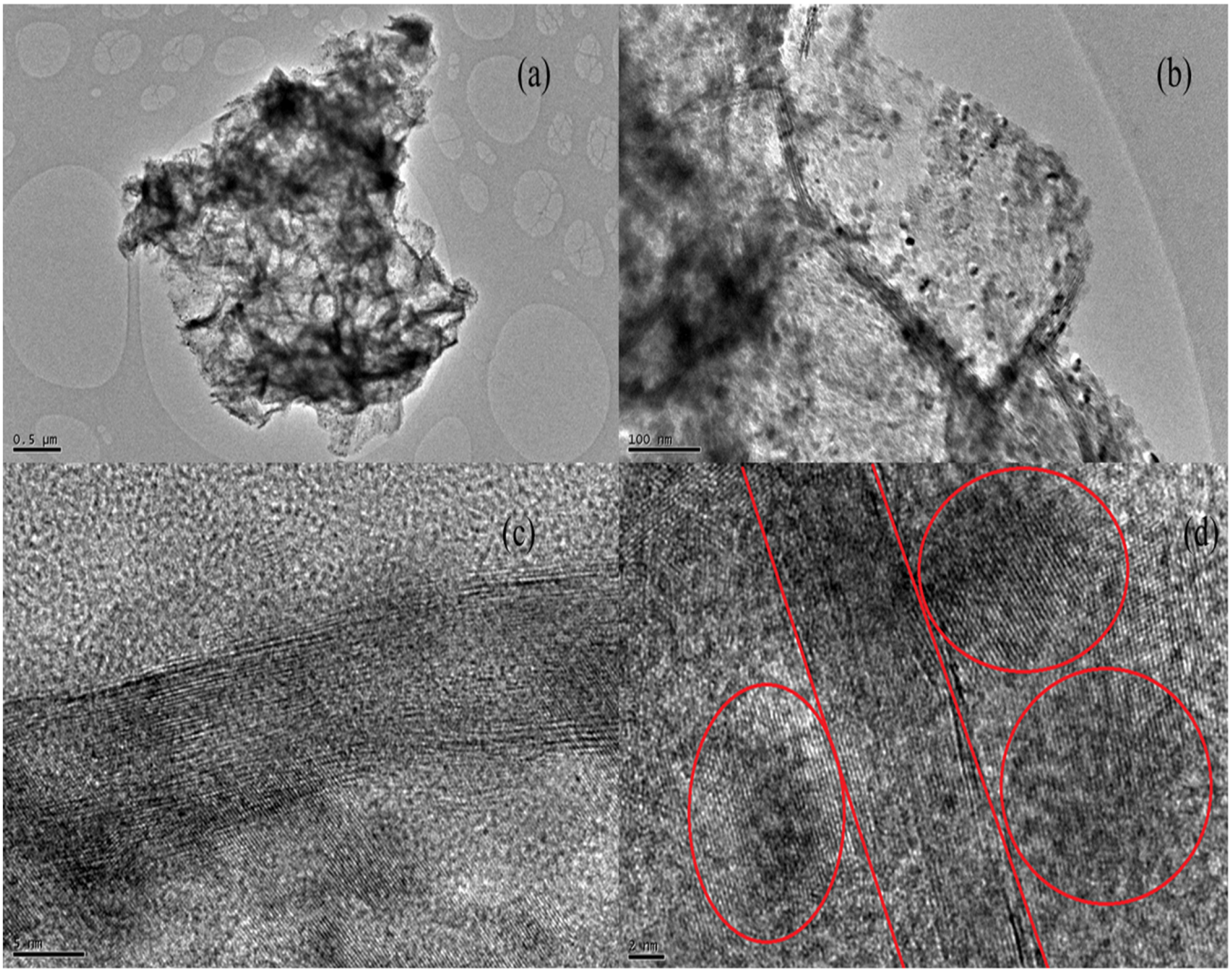

Figure 5. (a, b) Bright field TEM images and (c, d) HRTEM images of the hybrid material generated from reductive decomposition of adamantanecarboxylate intercalated Mg-Al layered double hydroxide (resultant nanocarbon wires/chains and MMOs are highlighted in image d). Scale bars in the images (a) 500 nm, (b) 100 nm, (c) 5 nm, and (d) 2 nm.

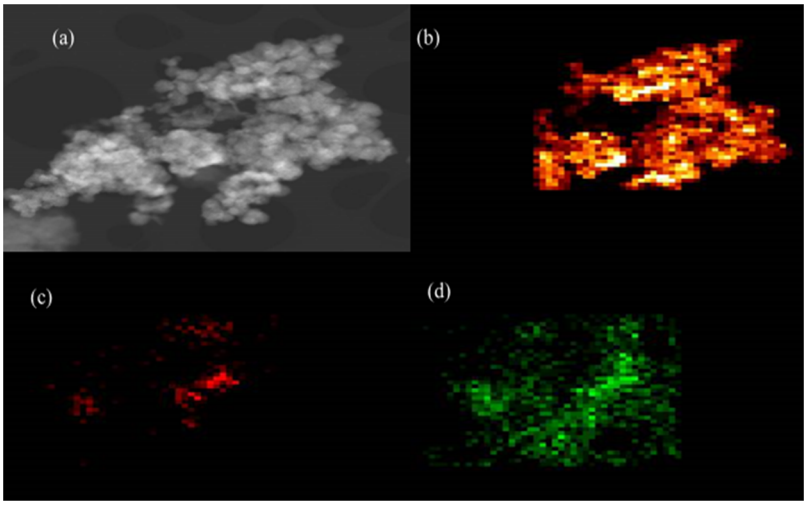

Figure 6. STEM elemental mapping images: (a) electronic image, (b) magnesium, (c) aluminum, and (d) carbon of the hybrid material generated from reductive decomposition of adamantanecarboxylate intercalated Mg-Al LDH.

DOI: 10.1021/acsomega.9b02534
ACS Omega 2019, 4, 20230−20236

using SEM, with all images obtained with a Hitachi SU-70 FEG SEM. The TEM and HRTEM imaging was undertaken using a JEOL 2100F FEG TEM. The metal content was established using X-ray fluorescence (XRF) spectroscopy. The samples were provided as homogenized powders and weighed on a 1 mg balance. The samples (93.8 and 26.7 mg) were placed directly into a Pt 95%/Au 5% crucible. To this, a lithium borate flux was added until the total weight of each sample and flux was 6.6 g. Claisse brand high-purity flux was used containing 66.67% $Li_2B_4O_7$, 32.83% $LiBO_2$, and 5.0% LiI (releasing agent). The sample and flux were then mixed together using a wooden stirring implement and placed in a Claisse Le Neo Fluxer using the "Refractory Materials" fixed conditions. The mixture was brought to a temperature of 1065 °C and rocked during fluxing. The total fluxing time was 15 min, and the cooling time was 6 min. The fused beads were run on a Panalytical Zetium WDXRF with a 4 kW rhodium anode tube. The samples were analyzed using the Panalytical proprietary "Wroxi" calibration, and corrections were made for the variable weight of each sample. The analysis time for each sample was 340 s.

■ ASSOCIATED CONTENT

Supporting Information

The Supporting Information is available free of charge on the ACS Publications website at DOI: 10.1021/acsomega.9b02534.

PXRD, FTIR, solid-state NMR spectra (^1H and ^{13}C), SEM, and TEM images of Mg-Al-adamantanecarboxylate LD; FTIR, ^{27}Al NMR spectrum, and EDX spectrum of the hybrid MMOs supported on carbon (PDF)

■ AUTHOR INFORMATION

Corresponding Author

*E-mail: chris.greenwell@durham.ac.uk.

ORCID

Andrew Whiting: 0000-0001-8937-8445

H. Chris Greenwell: 0000-0001-5719-8415

Notes

The authors declare no competing financial interest.

■ ACKNOWLEDGMENTS

We acknowledge John Hall, Gasan Alabedi, and Abdullah Al Shahrani (all at Saudi Aramco) for useful discussions. The authors acknowledge financial support from Saudi Aramco 'Development of Nano-Drilling Fluids' DNA-MPE-005-12. Thanks are also due to Dr. Budhika Mendis at the G. J. Russell Electron Microscopy facility, Department of Physics, Durham University for helping in recording TEM and to the Durham Solid State NMR facility, Department of Chemistry, for recording NMR spectra. We thank Dr. Kamal Badreshany, Department of Archaeology, Durham University for running the XRF analysis. We also acknowledge Prof. Karl S. Coleman and Prof. Andy Beeby, Department of Chemistry, Durham University for helping in recording Raman spectra.

■ REFERENCES

(1) Ruiz-Hitzky, E.; Casal, B. Intracrystalline Complexation by Crown Ethers and Cryptands in Clay Minerals. In. *Chemical Reactions in Organic and Inorganic Constrained Systems*; Setton, R., Ed.; NATO ASI Series (Series C: Mathematical and Physical Sciences), Springer: Dordrecht, 1986, *165*, 179−189.

(2) Dresselhaus, M. S.; Dresselhaus, G. Intercalation compounds of graphite. *Adv. Phys.* **2002**, *51*, 1−186.

(3) Bergbreiter, D. E.; Killough, J. M. Reactions of potassium-graphite. *J. Am. Chem. Soc.* **1978**, *100*, 2126−2134.

(4) Lagaly, G.; Beneke, K. Intercalation and exchange reactions of clay minerals and non-clay layer compounds. *Colloid Polym. Sci.* **1991**, *269*, 1198−1211.

(5) García-Ponce, A. L.; Prevot, V.; Casal, B.; Ruiz-Hitzky, E. Intracrystalline reactivity Of layered double hydroxides: carboxylate alkylations in dry media. *New J. Chem.* **2000**, *24*, 119−121.

(6) Mallouk, T. E.; Gavin, J. A. Molecular Recognition in Lamellar Solids and Thin Films. *Acc. Chem. Res.* **1998**, *31*, 209−217.

(7) Thompson, M. E. Use of Layered Metal Phosphonates for the Design and Construction of Molecular Materials. *Chem. Mater.* **1994**, *6*, 1168−1175.

(8) Zhu, Y.-P.; Ma, T.-Y.; Liu, Y.-L.; Ren, T.-Z.; Yuan, Z.-Y. Metal phosphonate hybrid materials: from densely layered to hierarchically nanoporous structures. *Inorg. Chem. Front.* **2014**, *1*, 360−383.

(9) Mitchell, K.; Ibers, J. A. Rare-Earth Transition-Metal Chalcogenides. *Chem. Rev.* **2002**, *102*, 1929−1952.

(10) Zhou, X.; Wilfong, B.; Vivanco, H.; Paglione, J.; Brown, C. M.; Rodriguez, E. E. Metastable Layered Cobalt Chalcogenides from Topochemical Deintercalation. *J. Am. Chem. Soc.* **2016**, *138*, 16432−16442.

(11) Jones, C. W.; Tsuji, K.; Davis, M. E. Organic-functionalized molecular sieves as shape-selective catalysts. *Nature* **1998**, *393*, 52−54.

(12) Poojary, D. M.; Zhang, B.; Clearfield, A. Pillared Layered Metal Phosphonates. Syntheses and X-ray Powder Structures of Copper and Zinc Alkylenebis (phosphonates). *J. Am. Chem. Soc.* **1997**, *119*, 12550−12559.

(13) Zhao, X.; Ando, Y.; Liu, Y.; Jinno, M.; Suzuki, T. Carbon Nanowire Made of a Long Linear Carbon Chain Inserted Inside a Multiwalled Carbon Nanotube. *Phys. Rev. Lett.* **2003**, *90*, 187401.

(14) Sanchez, C.; Belleville, P.; Popall, M.; Nicole, L. Applications of advanced hybrid organic−inorganic nanomaterials: from laboratory to market. *Chem. Soc. Rev.* **2011**, *40*, 696−753.

(15) Huang, L.; Chen, D.; Ding, Y.; Feng, S.; Wang, Z. L.; Liu, M. Nickel−Cobalt Hydroxide Nanosheets Coated on NiC-o_2O_4Nanowires Grown on Carbon Fiber Paper for High-Performance Pseudocapacitors. *Nano Lett.* **2013**, *13*, 3135−3139.

(16) Tang, Z.; Tang, C.-h.; Gong, H. A High Energy Density Asymmetric Supercapacitor from Nano-architectured $Ni(OH)_2$/Carbon Nanotube Electrodes. *Adv. Funct. Mater.* **2012**, *22*, 1272−1278.

(17) Zhao, M.-Q.; Zhang, Q.; Huang, J.-Q.; Wei, F. Hierarchical Nanocomposites Derived From Nanocarbons and Layered Double Hydroxides - Properties, Synthesis, and Applications. *Adv. Funct. Mater.* **2012**, *22*, 675−694.

(18) Zhong, H.-x.; Zhang, Q.; Wang, J.; Zhang, X.-b.; Wei, X.-l.; Wu, Z.-j.; Li, K.; Meng, F.-l.; Bao, D.; Yan, J.-m. Engineering Ultrathin C_3N_4 Quantum Dots on Graphene as a Metal Free Water Reduction Electrocatalyst. *ACS Catal.* **2018**, *8*, 3965−3970.

(19) Liu, K.-H.; Zhong, H.-X.; Yang, X.-Y.; Bao, D.; Meng, F.-L.; Yan, J.-M.; Zhang, X.-B. Composition-tunable synthesis of "clean" syngas via a one-step synthesis of metal-free pyridinic N-enriched self-supported CNTs: the synergy of electrocatalyst pyrolysis temperature and potential. *Green Chem.* **2017**, *19*, 4284−4288.

(20) LeBaron, P. C.; Wang, Z.; Pinnavaia, T. J. Polymer-layered silicate nanocomposites: an overview. *Appl. Clay Sci.* **1999**, *15*, 11−29.

(21) Miyata, S. Physico-chemical properties of synthetic hydrotalcites in relation to composition. *Clays Clay Miner.* **1980**, *28*, 50−56.

(22) Cavani, F.; Trifirò, F.; Vaccari, A. Hydrotalcite-type anionic clays: Preparation, properties and applications. *Catal. Today* **1991**, *11*, 173−301.

DOI: 10.1021/acsomega.9b02534
ACS Omega 2019, 4, 20230−20236

(23) Duan, X.; Evans, D. G. Layered double hydroxides. In. *Structure and Bonding*; Mingos, D. M. P., Ed.; Springer-Verlag: Berlin Heidelberg, 2006, pp. 1−233.
(24) Wang, Q.; O'Hare, D. Recent Advances in the Synthesis and Application of Layered Double Hydroxide (LDH) Nanosheets. *Chem. Rev.* **2012**, *112*, 4124−4155.
(25) Ma, R.; Sasaki, T. Nanosheets of oxides and hydroxides: Ultimate 2D charge-bearing functional crystallites. *Adv. Mater.* **2010**, *22*, 5082−5104.
(26) Hu, H.; Guan, B.; Xia, B.; Lou, X. W. Designed Formation of Co_3O_4/$NiCo_2O_4$ Double-Shelled Nanocages with Enhanced Pseudo capacitive and Electrocatalytic Properties. *J. Am. Chem. Soc.* **2015**, *137*, 5590−5595.
(27) Choudary, B. M.; Kantam, M. L.; Rahman, A.; Reddy, C. V.; Rao, K. K. The First Example of Activation of Molecular Oxygen by Nickel in Ni-Al Hydrotalcite: A Novel Protocol for the Selective Oxidation of Alcohols. *Angew. Chem., Int. Ed.* **2001**, *40*, 763−766.
(28) Choudhary, V. R.; Chaudhari, P. A.; Narkhede, V. S. Solvent-free liquid phase oxidation of benzyl alcohol to benzaldehyde by molecular oxygen using non-noble transition metal containing hydrotalcite-like solid catalysts. *Catal. Commun.* **2003**, *4*, 171−175.
(29) Debecker, D. P.; Gaigneaux, E. M.; Busca, G. Exploring, Tuning, and Exploiting the Basicity of Hydrotalcites for Applications in Heterogeneous Catalysis. *Chem. − Eur. J.* **2009**, *15*, 3920−3935.
(30) Fan, G.; Li, F.; Evans, D. G.; Duan, X. Catalytic applications of layered double hydroxides: recent advances and perspectives. *Chem. Soc. Rev.* **2014**, *43*, 7040−7066.
(31) Sideris, P. J.; Nielsen, U. G.; Gan, Z.; Grey, C. P. Mg/Al ordering in layered double hydroxides revealed by multinuclear NMR spectroscopy. *Science* **2008**, *321*, 113−117.
(32) Garcia-Gallastegui, A.; Iruretagoyena, D.; Gouvea, V.; Mokhtar, M.; Asiri, A. M.; Basahel, S. N.; al-Thabaiti, S. A.; Alyoubi, A. O.; Chadwick, D.; Shaffer, M. S. P. Graphene Oxide as Support for Layered Double Hydroxides: Enhancing the CO_2Adsorption Capacity. *Chem. Mater.* **2012**, *24*, 4531−4539.
(33) Garcia-Gallastegui, A.; Iruretagoyena, D.; Mokhtar, M.; Asiri, A. M.; Basahel, S. N.; al-Thabaiti, S. A.; Alyoubi, A. O.; Chadwick, D.; Shaffer, M. S. P. Layered double hydroxides supported on multi-walled carbon nanotubes: preparation and CO_2 adsorption characteristics. *J. Mater. Chem.* **2012**, *22*, 13932−13940.
(34) Meis, A. H.; Bitter, J. H.; De Jong, K. P. Support and Size Effects of Activated Hydrotalcites for Precombustion CO_2 Capture. *Ind. Eng. Chem. Res.* **2010**, *49*, 1229−1235.
(35) Othman, M. R.; Rasid, N. M.; Fernando, W. J. N. Mg−Al hydrotalcite coating on zeolites for improved carbon dioxide adsorption. *Chem. Eng. Sci.* **2006**, *61*, 1555−1560.
(36) Menzel, R.; Iruretagoyena, D.; Wang, Y.; Bawaked, S. M.; Mokhtar, M.; Al-Thabaiti, S. A.; Basahel, S. N.; Shaffer, M. S. P. Graphene oxide/mixed metal oxide hybrid materials for enhanced adsorption desulfurization of liquid hydrocarbon fuels. *Fuel* **2016**, *181*, 531−536.
(37) Zhang, S.; Fan, G.; Zhang, C.; Li, F. One-step synthesis of carbon nanotubes-copper composites for fabricating catalyst supports of methanol electrooxidation. *Mater. Chem. Phys.* **2012**, *135*, 137−143.
(38) Wang, G.; Chen, L.; Guan, S.; Zhang, X.; Wang, B.; Cao, X.; Yu, Z.; He, Y.; Evans, D. G.; Feng, J.; Li, D. Ultrathin and Vacancy-Rich CoAl-Layered Double Hydroxide/Graphite Oxide Catalysts: Promotional Effect of Cobalt Vacancies and Oxygen Vacancies in Alcohol Oxidation. *ACS Catal.* **2018**, *8*, 3104−3115.
(39) Li, X.; Sun, W.; Wang, L.; Qi, Y.; Guo, T.; Zhao, X.; Yan, X. Three-dimensional hierarchical self-supported $NiCo_2O4$/carbon nanotube core−shell networks as high performance supercapacitor electrodes. *RSC Adv.* **2015**, *5*, 7976−7985.
(40) Feng, J.; He, Y.; Liu, Y.; Du, Y.; Li, D. Supported catalysts based on layered double hydroxides for catalytic oxidation and hydrogenation: general functionality and promising application prospects. *Chem. Soc. Rev.* **2015**, *44*, 5291−5319.
(41) Zhong, H.-X.; Wang, J.; Zhang, Q.; Meng, F.; Bao, D.; Liu, T.; Yang, X.-Y.; Chang, Z.-W.; Yan, J.-M.; Zhang, X.-B. In Situ Coupling FeM (M = Ni, Co) with Nitrogen-Doped Porous Carbon toward Highly Efficient Trifunctional Electrocatalyst for Overall Water Splitting and Rechargeable Zn−Air Battery. *Adv. Sustainable Syst.* **2017**, *1*, 1700020.
(42) Meng, F.; Zhong, H.; Bao, D.; Yan, J.; Zhang, X. In Situ Coupling of Strung Co_4N and Intertwined N−C Fibers toward Free-Standing Bifunctional Cathode for Robust, Efficient, and Flexible Zn−Air Batteries. *J. Am. Chem. Soc.* **2016**, *138*, 10226.
(43) Zhang, J.; Feng, Y.; Ishiwata, H.; Miyata, Y.; Kitaura, R.; Dahl, J. E. P.; Carlson, R. M. K.; Shinohara, H.; Tománek, D. Synthesis and Transformation of Linear Adamantane Assemblies inside Carbon Nanotubes. *ACS Nano* **2012**, *6*, 8674−8683.
(44) Zhang, J.; Zhu, Z.; Feng, Y.; Ishiwata, H.; Miyata, Y.; Kitaura, R.; Dahl, J. E. P.; Carlson, R. M. K.; Fokina, N. A.; Schreiner, P. R.; Tománek, D.; Shinohara, H. Evidence of Diamond Nanowires Formed inside Carbon Nanotubes from Diamantane Dicarboxylic Acid. *Angew. Chem., Int. Ed.* **2013**, *52*, 3717−3721.
(45) Manohara, G. V.; Li, L.; Whiting, A.; Greenwell, H. C. Ultra-high aspect ratio hybrid materials: the role of organic guest and synthesis method. *Dalton Trans.* **2018**, *47*, 2933−2938.
(46) Khan, A. I.; Williams, G. R.; Hu, G.; Rees, N. H.; O'Hare, D. The intercalation of bicyclic and tricyclic carboxylates into layered double hydroxides. *J. Solid State Chem.* **2010**, *183*, 2877−2885.
(47) Nakamota, K. *Infrared and Raman spectroscopy of inorganic and coordination compounds*; Wiley: New York, 1986.
(48) Clark, C. B. x-ray diffraction data for compounds in the system cao-mgo-sio_2. *J. Am. Ceram. Soc.* **1946**, *29*, 25−30.
(49) Xu, X.; Wu, T.; Xia, F.; Li, Y.; Zhang, C.; Zhang, L.; Chen, M.; Li, X.; Zhang, L.; Liu, Y.; Gao, J. Redox reaction between graphene oxide and In powder to prepare In_2O_3/reduced graphene oxide hybrids for supercapacitors. *J. Power Sources* **2014**, *266*, 282−290.
(50) Rives, V. Study of Layered Double Hydroxides by thermal methods. In. *Layered Double Hydroxides: Present and future*; Rives, V., Ed.; Nova Science Publisher Inc.: New York, 2001, 127−151.
(51) Aramendía, M. A.; Avilés, Y.; Borau, V.; Luque, J. M.; Marinas, J. M.; Ruiz, J. R.; Urbano, F. J. Thermal decomposition of Mg/Al and Mg/Ga layered-double hydroxides: a Spectroscopic study. *J. Mater. Chem.* **1999**, *9*, 1603−1607.
(52) Das, A. K.; Srivastav, M.; Layek, R. K.; Uddin, M. E.; Jung, D.; Kim, N. H.; Lee, J. H. Iodide-mediated room temperature reduction of graphene oxide: a rapid chemical route for the synthesis of a bifunctional electrocatalyst. *J. Mater. Chem. A* **2014**, *2*, 1332−1340.

DOI: 10.1021/acsomega.9b02534
ACS Omega 2019, 4, 20230−20236